Double-Tiered Switched-Capacitor Battery Charge Equalization Technique

Andrew C. Baughman and Mehdi Ferdowsi, *Member, IEEE*

***Abstract*—The automobile industry is progressing toward hybrid, plug-in hybrid, and fully electric vehicles in their future car models. The energy storage unit is one of the most important blocks in the power train of future electric-drive vehicles. Batteries and/or ultracapacitors are the most prominent storage systems utilized so far. Hence, their reliability during the lifetime of the vehicle is of great importance. Charge equalization of series-connected batteries or ultracapacitors is essential due to the capacity imbalances stemming from manufacturing, ensuing driving environment, and operational usage. Double-tiered capacitive charge shuttling technique is introduced and applied to a battery system in order to balance the battery-cell voltages. Parameters in the system are varied, and their effects on the performance of the system are determined. Results are compared to a single-tiered approach. MATLAB simulation shows a substantial improvement in charge transport using the new topology. Experimental results verifying simulation are presented.**

***Index Terms*—Batteries, charge equalization, ultracapacitors.**

I. Introduction

ENERGY storage has been a critical component of any energy-related system [1], [2]. The automobile industry uses high-voltage battery and/or ultracapacitor packs in many of its new fully electric, hybrid electric, and plug-in hybrid vehicles [3], [4]. These packs can employ large high-voltage series strings of low-voltage storage units. As the pack is charged and discharged as a unit, individual cell temperature and internal chemistry characteristics can cause capacity imbalances in the form of voltage variations. Imbalanced cell voltages are caused by differences in cell capacities, internal resistances, chemical degradation, and intercell and ambient temperatures during charging and discharging. Any capacity imbalance between the modules can threaten the long-term reliability of the string as overall pack capacity is brought to the upper and lower limits of charge [5]–[9]. Imbalanced cell voltages can cause cell overcharging and discharging, decreasing the total storage capacity and lifetime of the unit. As both ultracapacitors and batteries suffer the same problems, only batteries will be mentioned here for clarity purposes.

For battery technologies used today, voltage plays a large part in determining state of charge of the battery. Given similar battery modules, one can attempt similar cycle-induced aging by making sure that the voltages of each battery in series are matched to the others. Many different solutions for controlling the battery state of charge through charge transport or protection have been proposed in the literature [10]–[20]. They use either capacitors, switches, or coupled or uncoupled inductors as a charge routing or storage device to shuttle energy between individual or groups of batteries.

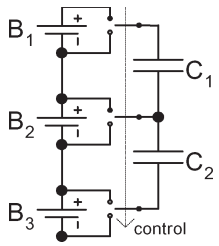

Fig. 1. Circuit diagram of single-tiered charge equalization method.

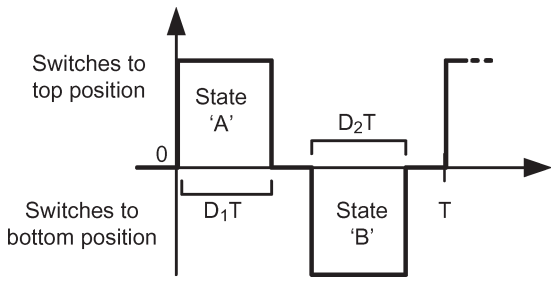

Fig. 2. Switching logic ($D_1 = D_2$).

One such charge transport device is a row of capacitors which are alternately connected to adjacent batteries, as shown in Fig. 1 [14]. In this method, hereafter referred to as single tiered, switches are controlled in unison, switching states back and forth between batteries at a fixed frequency without regard to state of charge. The advantages of this system are that no sensing or closed-loop control is needed and that the process is self-limiting: When voltage equalization is complete, the switching of the capacitors consumes minimal energy.

The switching logic for the capacitor's switches is shown in Fig. 2. For almost half of the switching period, the capacitors are connected through the switches to the upper batteries, which is called state "A," and then for the second half of the switching cycle, they are connected to the lower batteries, which is defined as state "B." There can be deadtime between the switching states to prevent shoot-through failure. Unlike the one shown in Fig. 2, its time length is much shorter than the switching period. Furthermore, it occurs after the steady state is established, and there is no charge transfer; therefore, there is no voltage

Manuscript received April 30, 2007; revised November 16, 2007. This work was supported by the National Science Foundation under Grant 0640636.

A. C. Baughman is with General Motors Corporation, Detroit, MI 48232-5170 USA.

M. Ferdowsi is with the Department of Electrical and Computer Engineering, Missouri University of Science and Technology, Rolla, MO 65409 USA.

Digital Object Identifier 10.1109/TIE.2007.918401

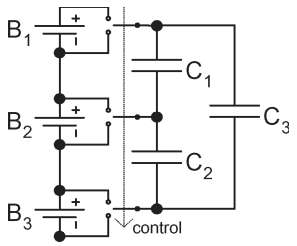

Fig. 3. Double-tiered method.

drop during the deadtime. The total switching period including deadtime is defined as "T" and is determined by the switching frequency by $1/f_{\text{switch}}$.

As shown in Fig. 3, a double-tiered method based upon the single-tiered work has been presented and shown to be an advancement upon the said method [21], [22]. In the new double-tiered method, a capacitor has been added to bridge the capacitors in the first row (or tier). With this advancement, batteries not directly connected to each other by a tier-1 capacitor now have another opportunity to exchange charge through the second-tier bridging capacitors. As a result, charge equalization time using the double-tiered method can be significantly reduced.

This paper describes the effects of circuit parameter variation on the effectiveness of charge transport for both the single- and double-tiered methods. A numerical approach is used due to the complexity of the system. Section II will discuss the derivation of the double-tiered equivalent circuit and equations, where Section III will bring up the methods for system analysis. Section IV discusses the effects of parameter variation on the system, and Section V discusses the ranges of the parameter variation whose results are shown in Sections VI–VIII. Section IX examines the effects of parameter variation on energy efficiency. Section X provides empirical data on the double- and single-tiered systems, which support the conclusion derived from simulation. Section XI draws conclusions and presents an overall evaluation of the new double-tiered charge equalization method.

II. Double-Tiered Equivalent Circuit Derivation

One metric which can be used to compare the effectiveness of the single- and double-tiered methods is the charge transported per switching cycle or, for a particular switching frequency, the average current transferred from one battery to another. To obtain this, an equivalent circuit model is required. The double-tiered circuit was first partially generalized such that all switch resistances were identical ("R"), all of the capacitor equivalent series resistances (ESRs) were identical ("r_c"), tier-1 capacitor values were identical and denoted by C_1 and C_2, tier-2 capacitance was denoted by C_3, and the batteries had no ESR. When the switches attain their A and B states and connect the capacitor network to different batteries, the equivalent circuit for each state is as shown in Fig. 4. The ESR of batteries is not completely neglected. Resistor R can also represent the ESR of the battery plus conduction resistance of the switch. However, it is not completely safe to say that the ESR of the battery is absorbed by "R."

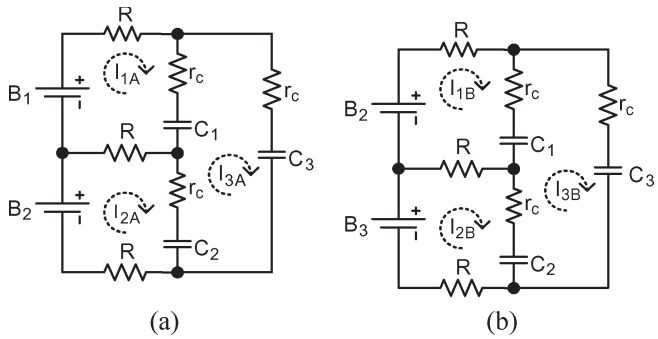

Fig. 4. Equivalent circuit showing mesh currents for states A and B.

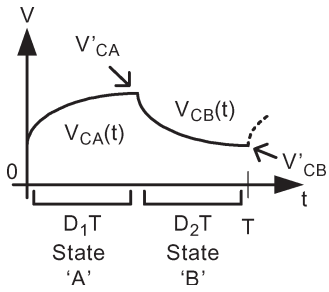

Fig. 5. Steady-state capacitor voltage waveform.

Mesh current equations for each state require system variables and the voltages of the capacitors at the end of the previous state. For this analysis, it is assumed that the converter is running in "steady state," or in other words, the initial voltages of the capacitors at system startup have been sufficiently dissipated or charged by converter action such that the voltage for any capacitor is mirrored from one switching cycle to the next. In this case, the ending voltage after time D_1T for the A state of any capacitor in the system is the starting voltage for that capacitor's B state, and the ending voltage after time D_2T for the B state is the beginning voltage of the A state (generically denoted by V'_{CA} and V'_{CB}, respectively), as shown in Fig. 5.

The mesh currents in the double-tiered method were expressed for both switch states in terms of their frequency-domain equivalents in (1), shown at the bottom of the next page.

The solutions for (1) can be turned into capacitor voltage equations in the frequency domain, as shown in the following:

$$\left\{\begin{array}{l} V_{C_{1A}}(s) = \frac{i_{1A}(s)-i_{3A}(s)}{s\cdot C_1} + \frac{V'_{C_{1B}}}{s} \\ V_{C_{2A}}(s) = \frac{i_{2A}(s)-i_{3A}(s)}{s\cdot C_2} + \frac{V'_{C_{2B}}}{s} \\ V_{C_{3A}}(s) = \frac{i_{3A}(s)}{s\cdot C_3} + \frac{V'_{C_{3B}}}{s} \\ V_{C_{1B}}(s) = \frac{i_{1B}(s)-i_{3B}(s)}{s\cdot C_1} + \frac{V'_{C_{1A}}}{s} \\ V_{C_{2B}}(s) = \frac{i_{2B}(s)-i_{3B}(s)}{s\cdot C_2} + \frac{V'_{C_{2A}}}{s} \\ V_{C_{3B}}(s) = \frac{i_{3B}(s)}{s\cdot C_3} + \frac{V'_{C_{3A}}}{s} \end{array}\right\}. \tag{2}$$

The voltage equations can then be converted into the time domain, where D_1T and D_2T are substituted in for time t for states A and B, respectively, to get the primed capacitor

voltages in terms of the previous state's primed voltages and circuit parameters. Simultaneous solving of six equations yields the primed voltages in terms of circuit parameters. With these voltages, the operation of the system in steady state is now known.

III. Analysis Equations

The charge transferred from battery to battery is carried through the capacitor tiers. More tiers means more paths between batteries, which yields less impedance to the transport of charge over a particular distance across the battery pack. In (3), the time-averaged current through any bridging capacitor path is calculated from its frequency, capacitor value, and its change in ending state voltages (voltage ripple). Even though the time-averaged current through any capacitor is zero, current enters the capacitor through one battery or one set of batteries and exits through another. In this manner, there is current using the capacitor as a path between batteries, [23], [24], heretofore known in this paper as "capacitor current"

$$\left\{\begin{aligned} I_C &= C\cdot\frac{\Delta V}{\Delta T} = C\cdot\left(\frac{\left(V'_{C_A}-V'_{C_B}\right)}{\frac{\Delta T}{2}} - \frac{\left(V'_{C_B}-V'_{C_A}\right)}{\frac{\Delta T}{2}}\right) \\ &= C\cdot f_{\text{sw}}\cdot\left(V'_{C_A}-V'_{C_B}\right) \end{aligned}\right\}. \quad (3)$$

The average current transferred to individual batteries comes from the shuttling capacitors which are connected to it, as shown in (4). For a single-tiered method, the current through the nonexistent (hence zero sized or value) C_3 would be zero

$$\left\{\begin{aligned} I_{B_1} &= I_{C_1}+I_{C_3} = f_{\text{sw}}\cdot\int_0^{D_1T} i_{1A}(t)dt \\ I_{B_2} &= -(I_{C_1}-I_{C_2}) = f_{\text{sw}}\cdot\left(\int_0^{D_1T} i_{2A}(t)dt + \int_0^{D_2T} i_{1B}(t)dt\right) \\ I_{B_3} &= -(I_{C_2}+I_{C_3}) = f_{\text{sw}}\cdot\int_0^{D_2T} i_{2B}(t)dt \end{aligned}\right\}. \quad (4)$$

These values will help in determining exactly how well the systems shuttle charge between batteries. Between these values and the effective capacitor current, one can figure out how much charge was received by the batteries and how it was transferred.

Energy efficiency is another metric by which one can compare the effectiveness of the single- and double-tiered methods. The efficiency of the charge transport is important; if a large amount of charge is lost for every unit transferred, it may not be worth shuttling the charge at all. The absolute computation of energy efficiency depends upon the direction of charge transport; however, the basic premise behind its calculation is the same, as shown in the following:

$$\text{energy efficiency} = \frac{\sum\begin{pmatrix}\text{energy}\\ \text{transferred}\end{pmatrix} - \sum\begin{pmatrix}\text{loss in passive}\\ \text{elements}\end{pmatrix}}{\sum\begin{pmatrix}\text{energy}\\ \text{transferred}\end{pmatrix}}. \quad (5)$$

In practical application, the energy efficiency can be calculated as the energy which was received at the recipient batteries versus the energy initially transmitted by the donor batteries, as shown in (6), with quantities derived from circuit parameters and (4)

$$\text{energy efficiency} = \frac{\sum\left(V_{B_{\text{received}}}\cdot I_{B_{\text{received}}}\right)}{\sum\left(V_{B_{\text{transmitted}}}\cdot I_{B_{\text{transmitted}}}\right)}. \quad (6)$$

"Losses" stemming from the initial charge transfer that is needed to energize the balancing capacitors are neglected due to their insignificant quantity when compared to the amount of charge that is transferred in normal operation over any practical length of runtime.

IV. Effects of Parameter Variation on Voltage Ripple

Each of the components of the balancing systems shown in Figs. 1 and 3 contributes to the end goal of charge balancing among batteries. To gain insight into how individual circuit parameters affect the response of the balancing system, it is necessary to pull out the variables in question and view their effects on charge transport. Equation (4) shows that the battery currents are sums of the capacitor-path currents. Equation (3) indicates that the average current over a switching cycle through a capacitor's path is a function of the switching frequency, capacitor value, and voltage ripple.

The contributions of the circuit parameters in the voltage-ripple component are not immediately obvious; the effects of circuit parameter variation on the voltage ripple shall be explored here. Although the constants presented in the succeeding sections may share names, they are distinct and separately derived variables.

$$\left\{\begin{aligned} \begin{bmatrix} i_{1A}\\ i_{2A}\\ i_{3A}\end{bmatrix} &= \begin{bmatrix} 2\cdot R + r_c + \frac{1}{s\cdot C_1} & -R & -r_c - \frac{1}{s\cdot C_1}\\ -R & 2\cdot R + r_c + \frac{1}{s\cdot C_2} & -r_c - \frac{1}{s\cdot C_2}\\ -\frac{1}{s\cdot C_1} - r_c & -\frac{1}{s\cdot C_2} - r_c & \frac{1}{s\cdot C_1}+\frac{1}{s\cdot C_2}+\frac{1}{s\cdot C_3}+3\cdot r_c\end{bmatrix}^{-1}\cdot\begin{bmatrix} V_{B_1}-V'_{C_{1B}}\\ V_{B_2}-V'_{C_{2B}}\\ V'_{C_{1B}}+V'_{C_{2B}}-V'_{C_{3B}}\end{bmatrix}/s \quad \text{state A}\\ \begin{bmatrix} i_{1B}\\ i_{2B}\\ i_{3B}\end{bmatrix} &= \begin{bmatrix} 2\cdot R + r_c + \frac{1}{s\cdot C_1} & -R & -r_c - \frac{1}{s\cdot C_1}\\ -R & 2\cdot R + r_c + \frac{1}{s\cdot C_2} & -r_c - \frac{1}{s\cdot C_2}\\ -\frac{1}{s\cdot C_1} - r_c & -\frac{1}{s\cdot C_2} - r_c & \frac{1}{s\cdot C_1}+\frac{1}{s\cdot C_2}+\frac{1}{s\cdot C_3}+3\cdot r_c\end{bmatrix}^{-1}\cdot\begin{bmatrix} V_{B_2}-V'_{C_{1A}}\\ V_{B_3}-V'_{C_{2A}}\\ V'_{C_{1A}}+V'_{C_{2A}}-V'_{C_{3A}}\end{bmatrix}/s \quad \text{state B}\end{aligned}\right\} \quad (1)$$

A. Battery Voltage

When the capacitor voltage ripples are examined and simplified with respect to battery voltage, a linear relationship is discovered, as shown in (7). The proportional variables are generated from circuit parameters. The voltage ripples are proportional to the difference between the batteries or charge sources to be equalized. This is as expected in an RC system; with all other things being equal, a higher voltage imbalance will yield a larger capacitor inrush current, which is, in this case, a battery balancing current. A special case of (7) occurs when $C_1 = C_2 = C_3$, $\alpha = \beta = \gamma$, and $\delta = 0$

$$\left\{ \begin{array}{l} \Delta V_{C1} = \alpha \cdot V_{B1} - \beta \cdot V_{B2} - \delta \cdot V_{B3} \\ \Delta V_{C2} = \delta \cdot V_{B1} + \beta \cdot V_{B2} - \alpha \cdot V_{B3} \\ \Delta V_{C3} = \gamma \cdot V_{B1} - \gamma \cdot V_{B3} \end{array} \right\}. \tag{7}$$

B. Switch Resistance

The contribution of switch resistance to the voltage ripple is more complex than the battery voltages'. Being an RC network, solving with respect to the switch resistance yields exponentials with "R" in the exponent. Equation (8) shows a breakdown of the nature of the relationship of switch resistance to voltage ripple when all shuttling tiers are equal in value

$$\Delta V_{C_n} = \alpha_n \cdot \left(\frac{1 - e^{-\frac{\beta}{1+\gamma \cdot R}}}{1 + e^{-\frac{\beta}{1+\gamma \cdot R}}} \right). \tag{8}$$

This special-case scenario is displayed here because the generic case is too complicated to clearly explain. For (8), α is independent of each of the shuttling capacitors, whereas β and γ are individual values which are identical between shuttling capacitors. α changes with varying battery voltages, β changes for nearly every system parameter except battery voltage, and γ appears to vary only with varying r_c. When the balancing capacitors or the duty cycles are not identical in value, the voltage ripple becomes a complicated expression that contains the summation of many exponentials and polynomials containing the switch resistance and does not yield intuitively obvious results.

C. Duty Cycle and Switching Frequency

Among the easiest system parameters to vary are the switching frequency and duty cycle. For each of the balancing capacitors, the voltage ripple is described by (9). The variable α changes with varying battery voltage and switch resistance, whereas the variable β varies with resistance and capacitance values. This equation is only valid in this simplified form for matching tier capacitances

$$\Delta V_{C_n} = \alpha_n \cdot \left(\frac{e^{-\beta \cdot D_1 \cdot T} + e^{-\beta \cdot D_2 \cdot T} - e^{-\beta \cdot (D_1 + D_2) \cdot T} - 1}{e^{-\beta \cdot (D_1 + D_2) \cdot T} - 1} \right). \tag{9}$$

V. Parameter Variation Testing

The effects of parameter variation are not entirely intuitively obvious when simply looking at the previous section, and some parameters are not covered due to the complexity of the resulting symbolic expression. Numerical analysis is simple to achieve and shall be carried forth herein. A simulation of the single- and double-tiered balancing setups in Figs. 1 and 3 was created. The parameters, or elements, of the circuit were changed for each simulation while holding all other parameters constant. The "standard-circuit" values from which parameters were varied and the parameter ranges were as in Table I.

TABLE I
Parameter Variation

Parameter	Range	Standard
Frequency	100 Hz to 1Mhz	50 kHz
R_{switch}(R)	1 mΩ to 10Ω	0.1Ω
Capacitor ESR (r_c)	–	0.1Ω
C_1, C_2	–	20 μF
C_3	0.1μF to 1mF	20 μF

The parameter variation range was chosen to cause the circuit to exhibit the effects of diminishing returns upon parameter variation for both the upper and lower ranges of values. Because the amount of charge transferred per switching cycle is also a function of the voltage difference between batteries, as shown in (7), the battery voltages were set to voltages of $V_{B1} = 3.5$ V and $V_{B2} = V_{B3} = 3$ V so that charge-advancing effects of current being transferred beyond a battery pair of zero voltage difference could be examined directly and easily. Other combinations of battery voltages cause alternate capacitor and battery current patterns to emerge; however, they are all intuitively derived from the results given.

Each parameter of the system, which is varied, produces an effect upon the total charge transport. Some parts, such as the ESR of the capacitors, have no interesting effect upon the system other than to move the crossover point (discussed later) to a different frequency or, in the case of the battery voltages or tier capacitances, to alter the system's efficiency. While these effects are important to the designer, they are predictable and shall be omitted here for length reasons. In the next sections, explanation will be taken to several system components which cause the most changes in the system.

VI. Analysis of Varying Switching Frequency

A simulation was run for the three-battery circuit in Figs. 1 and 3 where the circuit values were standard and the switching frequency was varied according to the range in Table I. Average capacitor current and average battery current were plotted versus varying switching frequency for the reference single-tiered case and the double-tiered case.

A. Single-Tiered Results

As the switching frequency is increased from zero, the current, or charge transport over time for the single-tiered system, is a linear function of how many switching periods there are per second; the time constant of the capacitor network is much smaller than the switching period, so the capacitors are able to fully equalize with their adjacent batteries. As switching frequency increases to an appropriate range, the

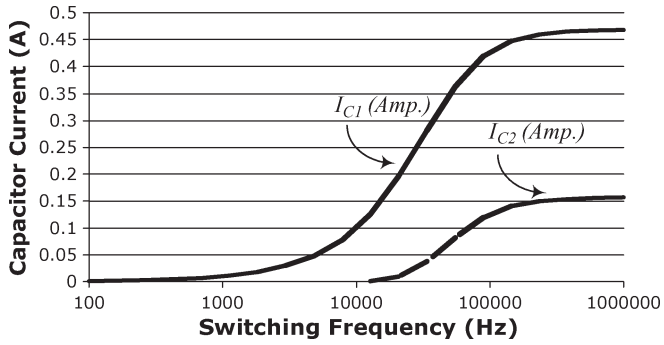

Fig. 6. Single-tier capacitor currents versus switching frequency.

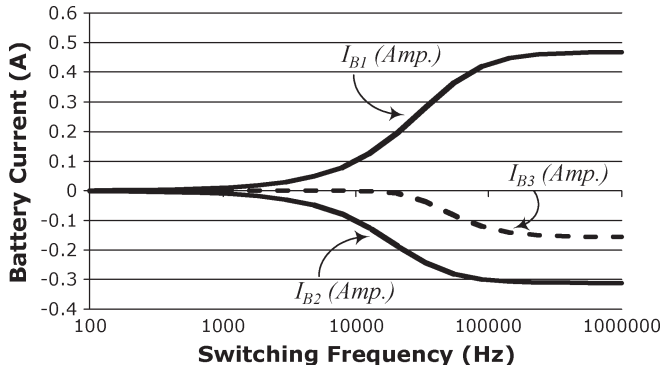

Fig. 7. Single-tier battery currents versus switching frequency.

capacitor equalization current is not able to fully die away, and so the average current raises exponentially. This can be observed in Fig. 6; Fig. 7 shows the resulting average battery currents.

At this point, a charge-advancing effect similar to what will be seen with the double-tiered system kicks in. Previously, the switching frequency was low enough such that the capacitors were allowed to reach an equalized voltage state, which gives a set maximum amount of energy per switching cycle; the average current through the capacitor at that point was a linear function of the switching frequency. As switching frequency increases, the capacitors are not allowed to fully equalize before they are switched to the other battery. In the example tested in this section, there is a higher voltage battery in series with two identical and lower voltage batteries.

At lower frequencies, there is no charge transport between V_{B1} and V_{B2}. If C_1 is not allowed to fully equalize during the A state before it is switched, then the current which V_{B1} is using to charge up C_1 is creating a voltage drop across its switch resistances, one of which is shared with the other capacitor-battery loop. As that current charges up C_1, it creates a voltage on the middle switch's resistance, which artificially inflates the apparent voltage of V_{B2} as seen by C_2. Charge then flows into that shuttling capacitor, and during the second half of the switching cycle, that energy is deposited into next battery, creating the charge-advancing effect which charges the third battery in the string within one switching cycle. This can be considered a "crossover" point for the single-tiered system, where the system moves charge farther than one battery per switching cycle.

At a high switching frequency where the time constant of the system is much larger than the on time of the duty cycle, the shuttling capacitors are unable to accumulate charge to an appreciable amount; the absolute value of the capacitor's current slows very little during the switching cycle. At this point, increasing the frequency would not increase the rate of charge transfer appreciably, as the current has already achieved its maximum value. This is shown in Fig. 6, where the capacitor current has reached a plateau with increasing frequency.

Predicting the behavior of the balancing system at low-enough frequencies that the charge-advancing phenomenon is not present is simple enough; however, it may be desired to predict the behavior of the circuit at high frequency. Instantaneously upon switching, the voltage difference between B_1 and C_1 in the A state at the start of the switching cycle can be considered to be spread across the three resistances in that loop: the capacitor's and two switch resistances. Therefore, in the standard-circuit scenario, a third of that voltage is across the switch resistance that bridges both mesh currents. That third of the original voltage drop is what creates the current in the second mesh.

This current relationship holds as long as the capacitors do not have the time to charge appreciably. By definition, the average current going into a capacitor in steady-state conditions is zero; thus, for this case, $|I_{1A}| = |I_{1B}|$ and $|I_{2A}| = |I_{2B}|$. Therefore, one knows that for the single-tiered case, the time-averaged current going through C_1 is also going through B_1, the time-averaged current going through C_2 is also going through B_3, and the difference between the two time-averaged currents is the time-averaged currents flowing through B_2. If $r_c = R$, then I_{B2} is two-thirds of I_1, and I_{B3} is one-third of I_1. More generally, see the following equation for the ratios of the capacitor and battery currents when the single-tiered method operates at an appropriately fast switching frequency after crossover

$$\left\{ \begin{array}{c} \frac{I_{C2}}{I_{C1}} = \frac{1}{2+\frac{r_c}{R}} \\ I_{B_1} = I_{C_1}, \quad I_{B_2} = I_{C_2} - I_{C_1}, \quad I_{B_3} = -I_{C_2} \\ \frac{I_{B2}}{I_{B1}} = -\left(\frac{1+\frac{r_c}{R}}{2+\frac{r_c}{R}}\right) \\ \frac{I_{B3}}{I_{B1}} = -\frac{1}{2+\frac{r_c}{R}} \end{array} \right\}. \quad (10)$$

B. Double-Tiered Results

Much of the same reasoning that was used in the single-tiered case can be used in the double-tiered case, with some exceptions. The double-tiered standard-circuit system exhibited a charge-transfer rate for C_1 that was not as high as that of the single-tiered method; nevertheless, here, C_3 carried a current that was identical to C_1, and C_2 carried no net current throughout the frequency range due to the identical tier capacitor values. At high frequencies above crossover, the total capacitor current transferred in both the single- and double-tiered systems was the same (see Figs. 6 and 8); however, an equal percentage of the total transferred current in the double-tiered case was advanced to B_2 and B_3, as opposed to the bulk being transferred to B_2 in the single-tiered method (see Fig. 6).

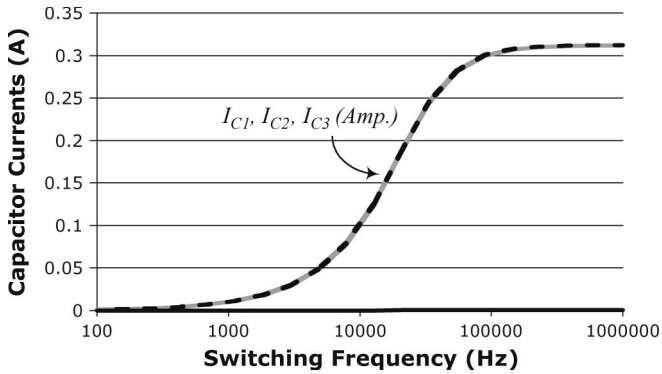

Fig. 8. Double-tier capacitor currents versus switching frequency.

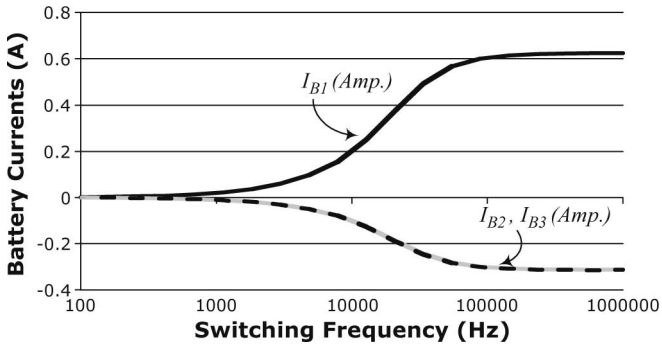

Fig. 9. Double-tier battery currents versus switching frequency.

This is the source of the speed of the double-tiered method. It can be seen from Figs. 7 and 9 that the current drawn from B_1 is higher in the double-tiered method than that of the single-tiered method because of the second path for charge to flow at any frequency. Both the single- and double-tiered systems experience approximately the same crossover frequency.

The reason that the charge-advancing effect that is visible in the single-tiered model does not appear here is because of the equal tier capacitance used in the simulation. Using the single-tier charge-advancing explanation as a model, when the system is in the A state, twice the current flows through the upper switch resistance as that of which flows through the two lower switch resistances. The mesh current that flows from B_1 to charge up C_1 returns through the middle-switch resistor and creates a polarity which increases V_{B2} relative to C_2; however, the current that flows from $(B_1 + B_2)$ to C_3 and then returns on the bottom-switch resistance creates a mesh current in the B_2, C_2 loop that has polarity of voltage across the middle-switch resistor that cancels the apparent voltage increase. The mesh current through the C_3 loop cancels out the current passing through C_2. Changing tier capacitance relative to the other tier would selectively increase or decrease the average current through C_2 and cause a change in Fig. 9.

By making a comparison between Figs. 7 and 9, one would observe that using a second tier of a capacitor will increase the average charging current of B_2 without having a drastic effect on the average currents of the other two batteries. Hence, the effectiveness of double-tiered method is not solely because it reduces the impedance and increases the current. It is mainly due to the provision of a better charge distribution between the charge donor and receiving batteries.

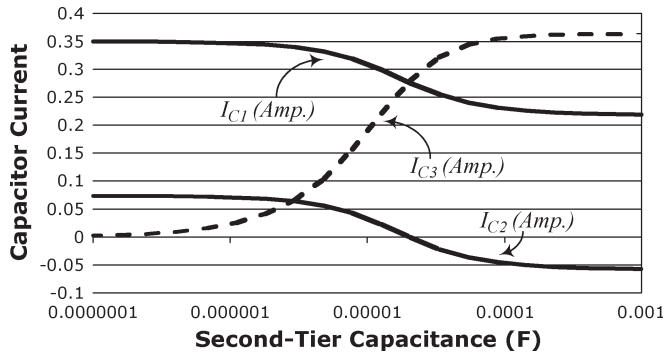

Fig. 10. Double-tiered capacitor currents versus tier-2 capacitance.

VII. Analysis of Varying Double-Tiered Capacitance

For the standard circuit described in Table I, the capacitance of the second tier was varied, and the effects upon the charge transport were recorded. In the previous section, the tier capacitances were equal, which canceled out the charge-advancing effect seen in the single-tiered method. When the double-tiered method is implemented and there are unequal tier capacitances, the charge-advancing effect becomes evident; the switching frequency used in the standard circuit places the system in the crossover frequency range, which will allow the system to show the effect.

Fig. 10 shows the currents of the balancing capacitors as the tier-2 capacitor is increased in value from effectively nothing to 1 mF. When the second tier is near zero, the system acts like a single-tier system and can be verified with Fig. 6 when evaluated at 50 kHz. As the second tier's capacitance is increased, current flow through the tier increases exponentially and then slows as the system enters a state where the second tier's capacitor can shuttle charge no faster. The current through the first tier decreases as the second tier's increases. As long as the second tier's capacitance value is less than or equal to that of the first tier, all capacitors work toward shuttling charge toward batteries of lower voltage. When the tier capacitances are equal, the capacitor current for C_2 reaches zero, and no charge-advancing effect is shown; this is as was discussed earlier. When the capacitance of the second tier exceeds the capacitance values of the first tier, C_2 begins to work against the progress of the system.

Fig. 11 shows the battery currents as the tier-2 capacitance is increased. When the second tier is not effectively present, the charge transferred to battery 3 is only that which is charge advanced; as the tier-2 capacitance increases, the current to battery 3 increases until the point where the tier capacitances are equal, which then provides an equal current to batteries 2 and 3. Current to battery 3 then exceeds battery 2 and levels off with increasing tier-2 capacitance. From the data in Fig. 11, there seems to be little benefit to increasing tier-2 capacitance beyond the level of tier-1 capacitances; however, this is due to the proximity of the standard circuit's switching frequency to the crossover point of the system. With a faster system time

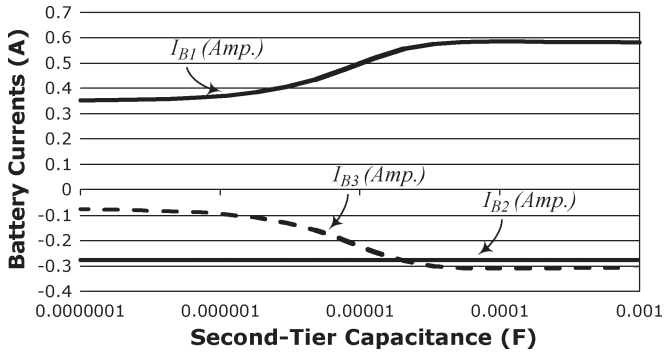

Fig. 11. Double-tier battery currents versus tier-2 capacitance.

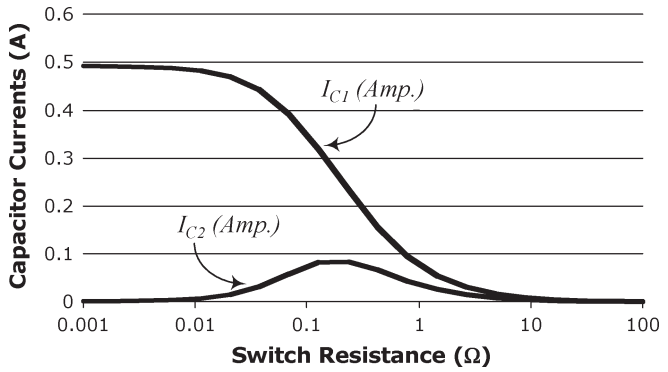

Fig. 12. Single-tier capacitor currents versus switch resistance.

constant or slower switching frequency, increasing C_3 beyond tier 1's value would continue to improve the capacitor's current level until crossover occurred.

VIII. Analysis of Varying Switch Resistance

For the standard circuit described in Table I, the switch resistance was varied, and the effects upon the charge transport were recorded. As stated earlier, switch resistance is the reason that the charge-advancement effect exists in the single-tier system; without it, there would be no mechanism to induce a charging current in the second balancing capacitor.

A. Single-Tiered Results

A single-tiered system, which has its switch resistance varied, produces a capacitor current response, as shown in Fig. 12. There seems to be an ideal value for the switch resistance if charge advancement alone in the single-tiered case is desired. For very low values of switch resistance, the current cannot develop a sufficient voltage across the switch resistance to significantly affect the second capacitor. If the resistance is too high, then the maximum transient capacitor current immediately upon switching is decreased; thus, the average value is also suppressed.

Fig. 13 shows the net result of the capacitor's work. The most current is propagated when the switch resistance is lowest; increasing the switch resistance increases the amount of current which reaches battery 3, but only to a point, and doing so significantly decreases the amount of current which can be transmitted to battery 2. From these results, it may be inferred

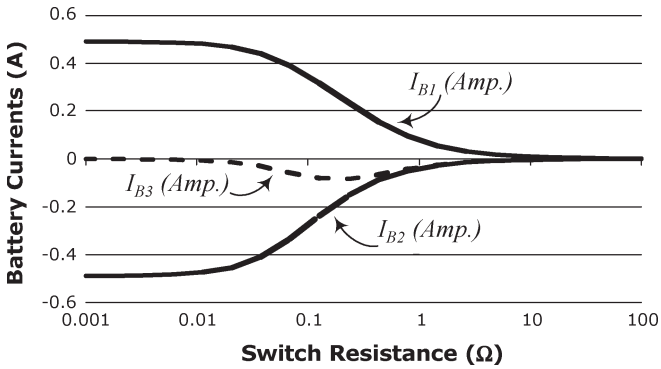

Fig. 13. Single-tier battery currents versus switch resistance.

that, although a charge-advancing option exists for a single-tiered system, a better result would be obtained by making an attempt to decrease the switch resistance.

B. Double-Tiered Results

With a double-tiered system, the designer has the option of choosing its tier-2 capacitance and thus has control over any switch resistance-created charge advancement. As noted in the single-tier results, increasing switch resistance decreases the rate of charge transport. The double-tiered system is superior to the single-tiered system in its ability to transport charge through the second tier, so there would be no reason to increase switch resistance for reasons of decreasing equalization time.

IX. Energy Efficiency

Energy efficiency is mainly governed by the voltage differences between the batteries which are to be equalized; as the batteries become equalized, the efficiency approaches 100%. Even so, other factors work to influence the efficiency levels for both the double- and single-tiered methods. Anything which changes the ratio of the system time constant to the switching period can affect the efficiency of the system. While the ratio is much greater or much less than one, the efficiency of the system is similar in its own local parameter range; however, when the ratio is in the vicinity of one-to-one, the efficiency will change from one asymptotic efficiency to another.

The efficiency of charging the capacitor in a simple RC circuit where the capacitor is initially discharged is 50%; this number grows if the starting voltage of the capacitor is elevated, approaching 100% when the capacitor's initial voltage approaches that of the voltage source.

In a switched capacitor system such as in Figs. 1 and 3, the situation grows quite complex. The charging of one of the capacitors affects the voltage swings of the other one or two balancing capacitors, which can alter the efficiency of the charge transfer. In the particular case of the system outlined in Section V, altering any of the system parameters besides the standard circuit voltages does not affect efficiency. Altering the voltages in any direction causes parameter variation to affect the energy efficiency of the charge transfer in ways described in the previous paragraphs; energy efficiency will move from one plateau to another, centering around the crossover point of any

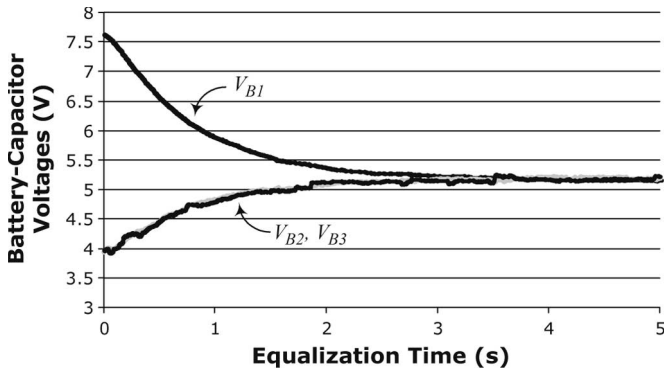

Fig. 14. Experimental results (double tier; $C_1 = C_2 = C_3 = 1\ \mu$F).

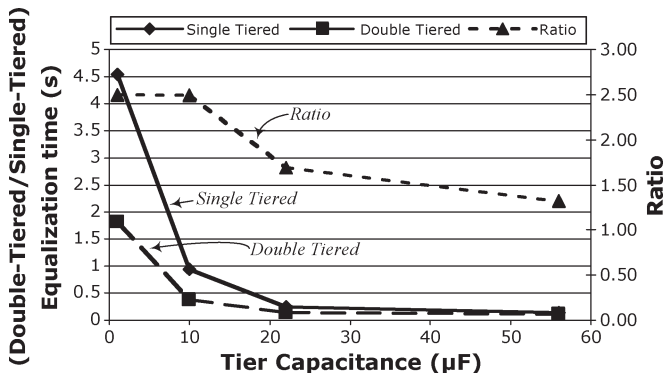

Fig. 15. Equalization time versus tier capacitance ($C_1 = C_2 = C_3$).

parameter's variation. When the voltage of B_2 rises between 3 and 3.25 V, increasing the ESR of the capacitors in a single-tiered system increases system efficiency although slightly; the effects are the same with decreasing switch resistance and switching frequency. With the double-tiered system in the standard-circuit configuration, energy efficiency is immobile with parameter variation other than changing battery voltages.

X. Experimental Verification

A system was created to experimentally verify equalization times for the single- and double-tiered methods. A setup of three 36-mF capacitors in series represented batteries to shorten the equalization time. Switches are implemented using power MOSFETs. The capacitors were initially balanced by using the balancing setup to be tested, then the balancing unit was deactivated. An end capacitor of the string of "battery" capacitors was then imbalanced a certain amount, and then the balancing units were reactivated. Data were taken until the voltage of the imbalanced capacitor fell to within 10% of its final balanced value. See Fig. 14 for a plot taken.

Single- and double-tiered systems were tested for 1-, 10-, 22-, and 56-μF balancing capacitors, where the double-tiered system had equal capacitance in its tiers. Results are in Fig. 15. The benefits of using a double-tiered balancer in a practical system seem to be diminishing with increasing capacitance. This could be due to parasitic effects brought about by using the larger capacitors, possibly due to its proximity to the system's crossover point.

The implementation cost of the double-tiered method is slightly more than that of the conventional approach. The extra cost is due to the addition of the second-tier capacitors; however, the first tier of capacitors, switches, and control circuitry remain the same. Fig. 15 is a good indicator of cost versus equalization-time tradeoff. It shows a four-times equalization-time decrease for only a 50% capacitance increase.

XI. Conclusion

Throughout the analytical and simulation results, it has been demonstrated that compared with the conventional single-tiered method, the double-tiered capacitive shuttling method is better at charge transport independent of component variations. It can be seen from the simulation graphs that the balancing capacitors in the double-tiered method suffer less from balancing currents than their the single-tiered counterparts while simultaneously transferring more charge further along the chain of batteries. This, along with decreased sensitivity to parameter variation, indicates that the double-tiered method is a suitable alternative to the standard single-tiered capacitor-based approach.

References

[1] Z. Jiang and R. A. Dougal, "A compact digitally controlled fuel cell/battery hybrid power source," *IEEE Trans. Ind. Electron.*, vol. 53, no. 4, pp. 1094–1104, Jun. 2006.

[2] S. Lemofouet and A. Rufer, "A hybrid energy storage system based on compressed air and supercapacitors with maximum efficiency point tracking (MEPT)," *IEEE Trans. Ind. Electron.*, vol. 53, no. 4, pp. 1105–1115, Jun. 2006.

[3] M. Ortuzar, J. Moreno, and J. Dixon, "Ultracapacitor-based auxiliary energy system for an electric vehicle: Implementation and evaluation," *IEEE Trans. Ind. Electron.*, vol. 54, no. 4, pp. 2147–2156, Aug. 2007.

[4] J. Moreno, M. E. Ortuzar, and J. W. Dixon, "Energy-management system for a hybrid electric vehicle, using ultracapacitors and neural networks," *IEEE Trans. Ind. Electron.*, vol. 53, no. 2, pp. 614–623, Apr. 2006.

[5] A. Affai, A. Bellini, G. Franceschini, P. Guglielmi, and C. Tassoni, "Battery choice and management for new-generation electric vehicles," *IEEE Trans. Ind. Electron.*, vol. 52, no. 5, pp. 1343–1349, Oct. 2005.

[6] H. Shibata, S. Taniguchi, K. Adachi, K. Yamasaki, G. Arlyoshi, K. Kawata, and K. Nishijima, "Management of serially-connected battery system using multiple switches," in *Proc. IEEE Int. Conf. Power Electron. Drive Syst.*, 2001, vol. 2, pp. 508–511.

[7] M. Bhatt, W. G. Hurley, and W. H. Wolfle, "A new approach to intermittent charging of valve-regulated lead-acid batteries in standby applications," *IEEE Trans. Ind. Electron.*, vol. 52, no. 5, pp. 1337–1342, Oct. 2005.

[8] Y. Lee and M. Cheng, "Intelligent control battery equalization for series connected lithium-ion battery strings," *IEEE Trans. Ind. Electron.*, vol. 52, no. 5, pp. 1297–1307, Oct. 2005.

[9] J. Chatzakis, K. Kalaitzakis, N. C. Voulgaris, and S. N. Manias, "Designing a new generalized battery management system," *IEEE Trans. Ind. Electron.*, vol. 50, no. 5, pp. 990–999, Oct. 2003.

[10] S. T. Hung, D. C. Hopkins, and C. R. Mosling, "Extension of battery life via charge equalization control," *IEEE Trans. Ind. Electron.*, vol. 40, no. 1, pp. 96–104, Feb. 1993.

[11] T. T. Sack, J. C. Tice, and R. Reynolds, "Segmented battery charger for high energy 28 V lithium ion battery," in *Proc. 16th Annu. Battery Conf. Appl. Adv.*, Jan. 2001, pp. 157–159.

[12] D. C. Hopkins, C. R. Mosling, and S. T. Hung, "The use of equalizing converters for serial charging of long battery strings," in *Proc. 6th Annu. Appl. Power Electron. Conf. Expo.*, Mar. 1991, pp. 493–498.

[13] Y. C. Hsieh, S. P. Chou, and C. S. Moo, "Balance discharging for series-connected batteries," in *Proc. Power Electron. Spec. Conf.*, 2004, vol. 4, pp. 2697–2702.

[14] C. Pascual and P. Krein, "Switched capacitor system for automatic series battery equalization," in *Proc. Modern Tech. Technol.*, 2000, pp. 57–59.
[15] Y. S. Lee, M. W. Chen, K. L. Hsu, J. Y. Du, and C. F. Chuang, "Cell equalization scheme with energy transferring capacitance for series connected battery strings," in *Proc. IEEE TenCON*, 2002, pp. 2042–2045.
[16] Y. S. Lee and G. T. Chen, "ZCS bi-directional DC-to-DC converter application in battery equalization for electric vehicles," in *Proc. IEEE Power Electron. Spec. Conf.*, Jun. 2004, vol. 4, pp. 2766–2772.
[17] C. S. Moo, Y. C. Hsieh, and I. S. Tsai, "Charge equalization for series-connected batteries," *IEEE Trans. Aerosp. Electron. Syst.*, vol. 39, no. 2, pp. 704–710, Apr. 2003.
[18] C. Karnjanapiboon, Y. Rungruengphalanggul, and I. Boonyaroonate, "The low stress voltage balance charging circuit for series connected batteries based on buck–boost topology," in *Proc. Int. Symp. Circuits Syst.*, May 25–28, 2003, vol. 3, pp. III-284–III-287.
[19] N. H. Kutkut, H. L. N. Wiegman, D. M. Divan, and D. W. Novotny, "Charge equalization for an electric vehicle battery system," *IEEE Trans. Aerosp. Electron. Syst.*, vol. 34, no. 1, pp. 235–246, Jan. 1998.
[20] Z. Ye and T. A. Stuart, "Sensitivity of a ramp equalizer on series batteries," *IEEE Trans. Aerosp. Electron. Syst.*, vol. 34, no. 4, pp. 1227–1236, Oct. 1998.
[21] A. C. Baughman and M. Ferdowsi, "Double-tiered capacitive shuttling method for balancing series-connected batteries," in *Proc. IEEE Veh. Power Propulsion Conf.*, Chicago, IL, Sep. 2005, pp. 50–54.
[22] A. C. Baughman and M. Ferdowsi, "Analysis of the double-tiered three-battery switched capacitor battery balancing system," in *Proc. IEEE Vehicle Power Propulsion Conf.*, Windsor, U.K., Sep. 2006, pp. 1–6.
[23] J. W. Kimball and P. T. Krein, "Analysis and design of switched capacitor converters," in *Proc. Appl. Power Electron. Conf. Expo.*, Mar. 2005, vol. 3, pp. 1473–1477.
[24] J. W. Kimball and P. T. Krein, "Modeling of capacitor impedance in switching converters," *IEEE Power Electron Lett.*, vol. 3, no. 4, pp. 136–140, Dec. 2005.

Andrew C. Baughman received the B.S. and M.S. degrees in electrical engineering from the University of Missouri, Rolla, in 2004 and 2006, respectively.

For his masters thesis, he performed research into battery charge equalization techniques, exploring ways to decrease equalization time while improving efficiency. He has been with General Motors Corporation, Detroit, MI, since 2006 as an Engineer in hybrid controls integration, working on energy storage systems.

Mehdi Ferdowsi (S'01–M'04) received the B.S. degree in electronics from the University of Tehran, Tehran, Iran, in 1996, the M.S. degree in electronics from Sharif University of Technology, Tehran, in 1999, and the Ph.D. degree in electrical engineering from the Illinois Institute of Technology, Chicago, in 2004.

He has been with the Department of Electrical and Computer Engineering, Missouri University of Science and Technology (MST), Rolla, as an Assistant Professor since August 2004. He has more than 35 publications in the areas of multi-input converters, multilevel converters, battery charge equalization techniques, hybrid vehicles, and digital control. His current research is focused on the integration of plug-in hybrid electric vehicles with electric power grid under a current NSF CAREER grant entitled "Vehicle Fleet as a Distributed Energy Storage System for the Power Grid."

Dr. Ferdowsi is an Associate Editor for the IEEE TRANSACTIONS ON POWER ELECTRONICS. He received the Joseph J. Suozzi INTELEC 2003 Fellowship Award from the IEEE Power Electronics Society. He also received MST's Outstanding Teaching Award in the 2005–2006 academic year.